

Model-based design approach to reducing mechanical vibrations

P. Czop ^a, G. Wszolek ^{b,*}

^a Department of Robotics and Mechatronics, AGH University of Science and Technology, Al. Mickiewicza 30, 30-059 Kraków, Poland

^b Institute of Engineering Processes Automation and Integrated Manufacturing Systems, Silesian University of Technology, ul. Konarskiego 18a, 44-100 Gliwice, Poland

* Corresponding e-mail address: grzegorz.wszolek@gmail.com

Received 11.05.2013; published in revised form 01.09.2013

Analysis and modelling

ABSTRACT

Purpose: The paper presents a sensitivity analysis method based on a first-principle model in order to reduce mechanical vibrations of a hydraulic damper.

Design/methodology/approach: The first-principle model is formulated using a system of continuous ordinary differential equations capturing usually nonlinear relations among variables of the hydraulic damper model. The model applies three categories of parameters: geometrical, physical and phenomenological. Geometrical and physical parameters are deduced from construction and operational documentation. The phenomenological parameters are the adjustable ones, which are estimated or adjusted based on their roughly known values, e.g. friction/damping coefficients.

Findings: The sensitivity analysis method provides major contributors and their magnitude that cause vibrations.

Research limitations/implications: The method accuracy is limited by the model accuracy and inherited nonlinear effects.

Practical implications: The proposed model-based sensitivity method can be used to optimize prototypes of hydraulic dampers.

Originality/value: The proposed sensitivity-analysis method minimizes a risk that a hydraulic damper does not meet the customer specification.

Keywords: Engineering design; Computer assistance in the engineering; Model-based design; First-principle model; Sensitivity analysis

Reference to this paper should be given in the following way:

P. Czop, G. Wszolek, Model-based design approach to reducing mechanical vibrations, Journal of Achievements in Materials and Manufacturing Engineering 60/1 (2013) 39-47.

1. Introduction

Recently, model-based design (MBD) approach in automotive industry is frequently used in design development cycle to find the best starting point for the design validation process using physical parts and prototypes [1-3]. MBD allows overcome the difficulties of traditional development process using comprehensive, first-principle

models that serve as executable specifications, replacing ambiguous text documents, and eliminating the need for physical prototypes before a mature design level is not achieved. Engineers can simulate and iterate as many times as necessary to refine the model to meet the constraints of the target product, and to validate the system behavior against the requirements building risk assessment scenarios. MBD facilities to ensure quality of the development process by integrating laboratory tests into the models at any stage. This continuous

verification process provides optimal prototype design understanding [4-7]. Another advantage is early error and contradictory requirements identification before any physical prototypes are machined and run through series of expensive tests.

This paper highlights fundamental challenges in reducing of vibration level of hydraulic dampers. The prototypes show frequently sensitivity to excite resonances and vibration interaction with other suspension components. The hydraulic damper performance is typically deteriorated in consequence of incorrect design parameters (e.g. topmount stiffness) and negative effects of physical phenomena such aeration and cavitation. These aspects are introduced and discussed in this section along the basic hydraulic damper operational principles and components characterization. Research work and experiments indicate that abnormal vibration of a hydraulic damper installed in passenger vehicles is related to high-frequency ranging from 50 to 500 Hz on the piston rod assembly, during the alternation of rod travel direction [8]. This paper focuses on a mathematical description of vibration transfer paths through the electro-mechanic-hydraulic system consisted of the servo-hydraulic tester and a hydraulic damper equipped with a topmount.

2. Formulation of the model

This section discusses necessary modifications of the variable damping hydraulic damper presented in [8] to formulate a double tube hydraulic damper model to be coupled to the servo-hydraulic model. The paper applies the same methodology; therefore the structure of the combined model (hydraulic damper + servo-hydraulic tester) remains the same. However, the parameters of the damper and tester are different since different units and laboratory setups were used in this study. The evaluation method of hydraulic damper vibrations referred to in this paper uses a servo-hydraulic tester to enable the transfer of random excitation to a hydraulic damper in the range 0-30 Hz, and to measure its response in the form of piston-rod acceleration in a broader range 0-500 Hz [8]. The type of considered hydraulic damper, Fig. 1, is a double-tube type consisting of three chambers, two of variable volumes (rebound and compression chambers) and one of fixed volume (reserve chambers). The chambers are connected by flow restrictions (orifices and valves).

The behavior of a hydraulic damper connected with a topmount can be described by the following equation:

$$m_{TM} \cdot \ddot{x}_{rod} + c_{TM} \cdot (\dot{x}_{rod} - \dot{x}_{TM}) + k_{TM} \cdot (x_{rod} - x_{TM}) = F_d \quad (1)$$

The force F_d generated by a hydraulic damper is obtained by taking the equilibrium of forces acting on the inertial piston-rod assembly into account:

$$F_d = p_{reb} \cdot A_{reb} + p_0 \cdot A_{rod} - p_{com} \cdot A_{com} + F_{fric} \quad (2)$$

where: A_{rod} , A_{com} , A_{reb} – the areas [m²] of the rod, compression and rebound side of the piston; p_{com} , p_{reb} – the pressures [Pa] in the compression and rebound chambers; p_0 – the atmospheric pressure $p_0=1e5$ [Pa]; F_{fric} – the dry friction force between the piston and pressure tube.

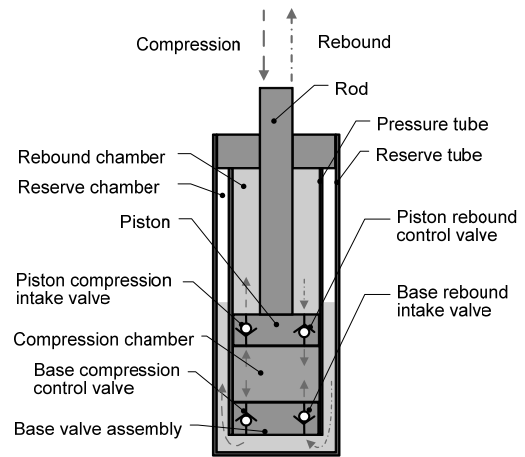


Fig 1. Hydraulic damper working principle

The dry friction force F_{fric} between the piston and pressure tube is modeled as follows:

$$F_{fric} = F_{fric_max} \cdot \tanh\left(\frac{\dot{x}_{tube} - \dot{x}_{rod}}{v_{ref}}\right) \quad (3)$$

where the friction force F_{fric} depends on the direction of relative velocity $(\dot{x}_{tube} - \dot{x}_{rod})$ of the piston-rod assembly and the body (tube) of the hydraulic damper [8]. The proposed friction model uses the hyperbolic tangent function $\tanh(\cdot)$ which provides a smooth switching of friction force similar to the measurement data. The maximum friction force F_{fric_max} is experimentally obtained using a hydraulic damper without valve restrictions for the low reference velocity $v_{ref}=0.01$ m/s.

The measured static pressure-flow characteristics of all restrictions are required in the model to capture the relationship between the pressure drop Δp across the considered valve assembly and the volumetric flow rate q through the valve assembly. The reference [8] shows pressure-flow characteristics which were measured on a flow-bench device and used in the model. Changes in the oil mass in the compression, rebound and third tube chambers are obtained using the following equations:

$$\begin{aligned} \begin{bmatrix} \dot{m}_{reb} \\ \dot{m}_{com} \end{bmatrix} &= \begin{bmatrix} (q_{piston,reb} - q_{piston,com}) \cdot \rho_{com,reb} & \dots \\ -(q_{piston,reb} - q_{piston,com}) \cdot \rho_{com,reb} & \dots \\ -q_{rg} \cdot \rho_{reb,emu_res} & \dots \\ \dots + (q_{cend,reb} - q_{cend,com}) \cdot \rho_{com,emu_res} \end{bmatrix} \end{aligned} \quad (4)$$

where \dot{m} , q , and ρ represent mass flow rate, volumetric flow rate, and density respectively. The density of the oil flowing through the valves is obtained as the average value of the oil density in the connected chambers. The maximum calculated change in the density of the oil is less than 0.35% if the differential pressure over the valve does not exceed 5 MPa [8]. Rearranging the mass flow equation and knowing that

$$\rho_{a,b} = \frac{1}{2} \cdot (\rho_a + \rho_b); \quad a, b = \{com, reb, emu_res\} \quad (5)$$

$$\rho_a = \frac{m_a}{V_a}; \quad a, b = \{com, reb\} \quad (6)$$

the following differential equations are obtained

$$\begin{aligned} \begin{bmatrix} \dot{m}_{reb} \\ \dot{m}_{com} \end{bmatrix} &= \dots \\ \dots &= \frac{1}{2} \mathbf{q} \cdot \begin{bmatrix} 1/V_{reb} & 0 \\ 0 & 1/V_{com} \end{bmatrix} \cdot \begin{bmatrix} m_{reb} \\ m_{com} \end{bmatrix} \dots + \\ \dots &+ \frac{1}{2} \cdot \begin{bmatrix} -q_{rg} \\ q_{cend,reb} - q_{cend,com} \end{bmatrix} \cdot \rho_{emu_res} \end{aligned} \quad (7)$$

where:

$$\mathbf{q} = \begin{bmatrix} q_{piston,com} - q_{piston,reb} - q_{rg} & \dots \\ -q_{piston,com} + q_{piston,reb} & \dots \\ & q_{piston,com} - q_{piston,reb} \\ \dots - q_{piston,com} + q_{piston,reb} + q_{cend,reb} - q_{cend,com} \end{bmatrix} \quad (8)$$

The volumes of the V_{com} compression and V_{reb} rebound chambers are obtained with the following algebraic formula:

$$V_{reb} = V_{reb_ini} + A_{reb} \cdot (x_{rod} - x_{tube}) \quad (9)$$

$$V_{com} = V_{com_ini} + A_{com} \cdot (x_{tube} - x_{rod}) \quad (10)$$

where $(x_{tube} - x_{rod})$ is the relative movement between the piston-rod assembly and the body of the hydraulic damper, V_{reb_ini} and V_{com_ini} are the rebound and compression chamber volumes at the displacement $x_{tube} - x_{rod} = 0$. The total oil mass in particular chambers is obtained as follows:

$$\begin{aligned} m_{reb} &= m_{reb_ini} + \int \dot{m}_{reb} dt \\ m_{com} &= m_{com_ini} + \int \dot{m}_{com} dt \end{aligned} \quad (11)$$

based on the initial oil mass and the mass changes in the rebound, compression and third tube chambers. The mass of the oil in the reserve chamber is calculated based on the oil mass balance of the entire hydraulic damper:

$$m_{res} = m_{oil} - m_{reb} - m_{com} \quad (12)$$

The average density of the oil-gas emulsion in the reserve chamber ρ_{emu_res} is a function of the average density of the oil-gas emulsion and gas in the reserve chamber ρ_{res} .

$$\rho_{emu_res} = f(\rho_{res}) \quad (13)$$

The average density ρ_{res} can be calculated with the formula

$$\rho_{res} = \frac{m_{gas_res} + m_{emu_res}}{V_{res}} \quad (14)$$

$$m_{emu_res} = m_{emu} - m_{reb} - m_{com} \quad (15)$$

where: m_{gas_res} - the mass of free gas in the reserve chamber [kg]; m_{emu_res} - the mass of the oil-gas emulsion in the reserve chamber [kg]; m_{emu} - the mass of the oil-gas emulsion in the whole double-tube damper [kg]; m_{reb} - the mass of the oil-gas emulsion in the rebound chamber [kg]; m_{com} - the mass of the oil-gas emulsion in the compression chamber [kg]; V_{res} - the volume of the reserve chamber [m³]; The volumetric flows q through the piston, cylinder-end and rod guide depend on the pressure drop Δp and are given as static characteristics.

$$\begin{aligned} q_{piston,com} &= f(\Delta p_{com,reb}); \\ q_{piston,reb} &= f(\Delta p_{reb,com}); \\ q_{cend,com} &= f(\Delta p_{com,res}); \\ q_{cend,reb} &= f(\Delta p_{res,com}); \\ q_{rg} &= f(\Delta p_{reb,res}); \end{aligned} \quad (16)$$

$$\Delta p_{a,b} = p_a - p_b; \quad a, b = \{com, reb, res\} \quad (17)$$

The pressures p_{com} , p_{reb} , p_{res} is determined as a function of density

$$p_a = f(\rho_a); \quad a = \{com, reb, res\} \quad (18)$$

The aeration effect is taken into account using the model developed in [8]. The model parameters are listed in Table 1.

Vibration evaluation is performed on the entire vehicle under road and laboratory conditions. However, it is also frequently performed on isolated systems of gradually increasing complexity in laboratory conditions, i.e. suspension or hydraulic damper level. This approach allows interactions with the vehicle body to be eliminated and then, in turn, test conditions to be more precisely controlled. Laboratory experiments are more repeatable than on-road driving sessions. It is also easier to simulate typical road manoeuvres and measure certain signals, such as tire forces, or use special measurement equipment. On the other hand, laboratory-based tests enable the reduction of costs and allow tests to be performed faster. Vibration tests performed on a servo-hydraulic tester are intended to quantify and rank the intensity of vibrations generated by hydraulic dampers [8].

The servo-hydraulic tester affects the evaluation of test results since the hydraulic actuator has a variable stiffness and specific resonance frequency. It is therefore necessary to include the servo-hydraulic tester dynamic by means of its model coupled to the hydraulic damper model. The hydraulic damper and the servo-hydraulic tester models are coupled via force, velocity and displacement feedback relations as presented in [8]. A hydraulic damper is rigidly attached to the main frame of the servo-hydraulic tester through a top fixation (the load cell) and a top

mount. The bottom end of the hydraulic damper is rigidly connected to the rod of the hydraulic actuator. The servo-tester model parameters are introduced in Table 2.

Table 1.
Parameters of the hydraulic damper model

Configuration parameters	Values
Physical	
bulk modulus of an oil K	1.6e9 [N/m ²]
ratio of the gas/oil mass ζ	1e-8 [-]
gas constant (nitrogen) R	8.31 [J/(mol/K)]
oil temperature T	309[K] (≈ 36 [°C])
total oil volume V_{oil}	390e-6 [m ³]
Geometry	
initial gas pressure p_{ini}	5e5 [Pa]
area of the rod section A_{rod}	380e-6 [m ²]
area of the piston section A_{com}	805e-6 [m ²]
initial volume of the rebound chamber V_{reb_ini}	81e-6 [m ³]
initial volume of the compression chamber V_{com_ini}	130e-6 [m ³]
volume of the reserve chamber V_{res}	311e-6 [m ³]
Components	
moving mass m_{TM} (top mount + piston-rod assembly mass)	1 [kg]

The equivalent system of the servo-hydraulic tester is formulated as a serial connection of mass, damping, and stiffness equivalent elements [4-5]. In this model, the coefficients representing the damping and stiffness of a hydraulic damper and a hydraulic actuator are nonlinear, and their values result from the nonlinear hydraulic flow equations presented in the previous sections.

3. Adjustment of a first-principle model

The first-principle hydraulic damper model requires a few physical parameters which are related to fluid (oil) properties affected by ambient conditions, e.g. oil density. Other physical parameters are provided in the form of parameter and characteristic, such as top mount stiffness or piston friction respectively. The fixed geometrical parameters are measured directly or taken from the customer specifications regarding the hydraulic actuator. The last category consists of the phenomenological parameters to which hydraulic leakages, gas/oil mass ratio, discharge and piston friction coefficients belong. These parameters are known only by their approximate values obtained at specific conditions, e.g. fixed ambient temperature. The hydraulic leakages over the piston are difficult to obtain without precise measurements due to unknown tube-piston tolerances. The leakages over the piston-rod assembly in hydraulic dampers are tunable and controlled using valve discs with calibrated orifices. The gas-oil mass ratio was roughly

calculated using Henry's equation [8] while the critical discharge coefficient of the servo-valve is the free parameter. A topmount is the external component attached to the hydraulic damper which transfers the rod force to the suspension. Its stiffness is obtained on a static load frame machine as a force-displacement characteristic. The damping of the topmount is, however, difficult to obtain without specialized measurements; therefore this parameter is a free one. The servo-hydraulic tester model uses a simplified model of a servo-valve reduced to the second-order transfer function representing the dynamics of the spool. The transfer function has two parameters, which are the natural frequency and damping ratio. The natural frequency is known, because the amplitude-phase-frequency characteristic of the servo-valve is available from the manufacturer, while the damping depends on usage of the valve and other factors (hydraulic forces), therefore it is a free parameter.

Table 2.
Parameters of the servo-hydraulic tester model

Configuration parameters	Values
PID controls	
proportional (P)	0.052
integral (I)	0.1
derivative (D)	0
feed-forward (FF)	0
Physical	
fluid bulk modulus	1.5e5 [MPa]
Geometry	
piston rod diameter	45 [mm]
volume chamber A and B	93.2e-6 [m ³]
area of piston side A and B	373 [mm ²]
piston mass	10 [kg]
oil temperature T	309[K] (≈ 36 [°C])
Phenomenological	
piston friction	10 [Ns/m]
chamber leak rate	10e-6 [cm ³ /s]

The advantage of the first-principle approach [9-10] is the possibility to apply physical boundaries to parameters to avoid local minimum regions during optimization. The PID settings are known as they are the test rig configuration parameters. The model parameters are adjusted using operational data as presented in Table 3.

The validation tests of the hydraulic damper model were conducted using the second-order method, i.e. Levenberg-Marquardt algorithms [11-12]. The sum of squared errors was used as the error criterion to evaluate the fit of the model to operational data in the frequency domain based on the rod damper acceleration [10]. The power spectrum was obtained using the common logarithm function with base 10 applied to acceleration signal sampled at the rate of 2kHz and processed with an FFT

(Fast Fourier Transform) algorithm where the Hamming window length is 512 samples and the overlap parameter is set to 50%. The objective function is defined as follows:

$$\varepsilon(\omega, \theta) = \log_{10}[y(\omega)] - \log_{10}[g(\omega; \theta)] \quad (19)$$

Table 3. Adjustable parameters of the model.

Parameter	Unit	Min value	Max value	Estimated Value
Topmount damping coefficient c_{TM}	[N/s]	0.5	50	44.75
Discharge coefficient of the servo-valve	[-]	0.1	0.6	0.55271
Equivalent damping ratio of the servo-valve	[-]	0.5	5	1.6881
The area of leakage between the upper and the lower chamber of the actuator	[m ²]	1e-13	1e-9	9.7139e-10

Table 3 shows the evaluation results of different algorithms for the stopping criterion chosen as the exceeded number of iterations or approached stable value for the parameters, i.e. the difference between the current and the previous value is zero. The quality of the model fit is assessed by a measure based on the Pearson correlation coefficient. The results that provide the best trade-off between data fit to operational data and calculation time were achieved for the second-order method within the 12 iterations, while the worst results were for the first-order method. The best results obtained for the second-order method are presented in Fig. 2.

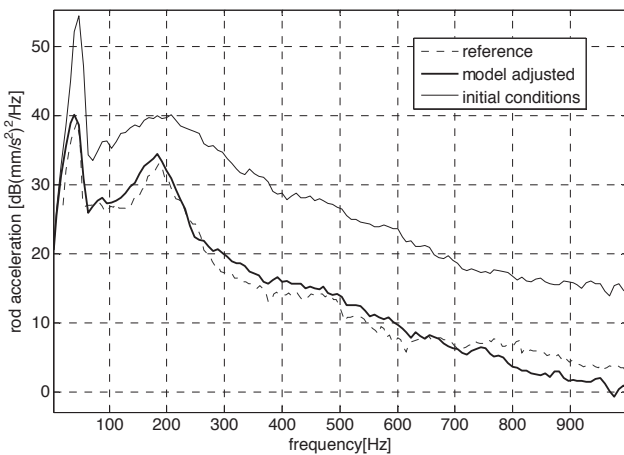


Fig. 2. The response of the hydraulic damper model vs. measurements in the frequency domain

The model was initially calibrated based on the available a priori knowledge; the initial values of phenomenological parameters were assumed based on similar damper construction.

Fig. 2 shows the model accuracy for those initial conditions and after the adjustment process. The best results obtained for the second-order method are also presented in Fig. 3 to show the acceleration signal directly in time domain.

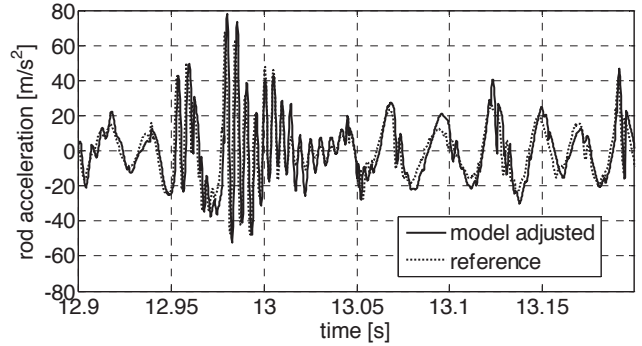


Fig. 3. Model response vs. operational measurements in time domain

The convergence of the Newton-Gauss algorithm was visually inspected by clear trends in sequences of the parameter values illustrating the speed in which the algorithm approaches the adjusted value. The convergence trajectory plots and the cost function plot showed trends towards constant values of the parameters and cost function, which correspond to convergence towards the minimum of the criterion function, within 12 iterations.

4. Sensitivity analysis method

The proposed first-principle model-based sensitivity analysis [13-15] allows to quantify the influence of geometrical and physical parameters on vibration level of a hydraulic damper based on the laboratory tests. The analysis uses a Pareto diagram which is scaled to show the positive or negative parameter value effect in the frequency domain. The model response was generated based on the input matrix (Table 4). The parameter sensitivity ranges are defined using maximal and minimal parameter values for two operating ranges, namely narrow around the operating point (low) and broader out of the operating point (high).

The obtained PSD (Power Spectral Density) values are normalized using the following metric:

$$\Delta A_i = A_{i,max} - A_{i,min} \quad (20)$$

where $A_{i,max}$ and $A_{i,min}$ are the PSD amplitudes obtained respectively for the maximal and minimal value. The influence factors are normalized within the range (-100%; 100%) at every considered frequency bin.

$$w_i = \frac{\Delta A_i}{\sum_{i=1...N} abs(\Delta A_i)} \quad (21)$$

Table 4.
Parameters considered for the numerical experiment

No.	Parameter Category	Parameter (factor)	Parameter value						Unit
			min		nominal		max		
			low	high	low	high	low	high	
1	Internal	Rod diameter	0.9	N/A	1	1	1.1	N/A	[m]
2		Pressure tube diameter	0.9	N/A	1	1	1.1	N/A	[m]
3		Oil level	0.9	0.7	1	1	1.1	1.3	[m ³]
4		Aeration (gas/oil mass ratio)	0.9	0.7	1	1	1.1	1.3	[-]
5		Compression base valve characteristic	0.9	0.7	1	1	1.1	1.3	[m ³ /min]
6		Rebound base valve characteristic	0.9	0.7	1	1	1.1	1.3	[m ³ /min]
7		Compression piston valve characteristic	0.9	0.7	1	1	1.1	1.3	[m ³ /min]
8		Rebound piston valve characteristic	0.9	0.7	1	1	1.1	1.3	[m ³ /min]
9	External	Stiffness of the topmount k_{TM}	0.9	0.7	1	1	1.1	1.3	[N/m]

The normalized values are displayed in the sensitivity diagram where positive influence values increasing the PSD values, while the negative decreasing the PSD values (Fig. 4).

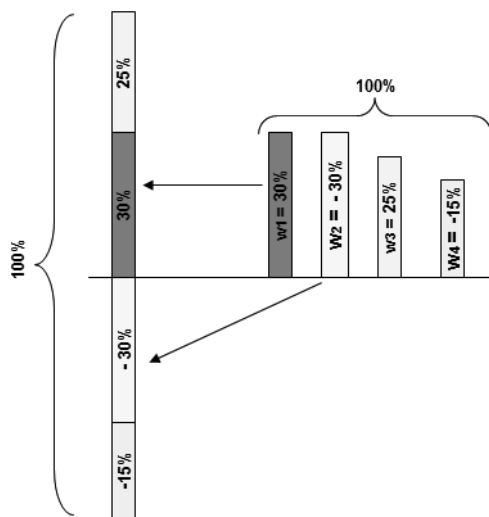


Fig. 4. Graphical interpretation of vibration contributors

The contributors are graphically interpreted as Pareto graphs obtained at each frequency bin or interval.

The analysis is conducted independently assuming small perturbation around the operating point ($\pm 10\%$) or assuming more significant influence for $\pm 30\%$ change in a parameter value.

The low-range (10%) sensitivity analysis shows that rod-bore diameter of a hydraulic damper has significant impact on vibration level compare to other contributors (Fig. 5). This effect dominates since the contribution of rod and bore diameter achieves 80%. The effect has dual influence, namely increasing and decreasing the vibration level measured at the piston-rod assembly. The second important contributor is the stiffness of the topmount. Moderate influence shows aeration (gas/oil mass ratio) and oil volume inside the internal pressure. The less influence results from valve system spring stiffness.

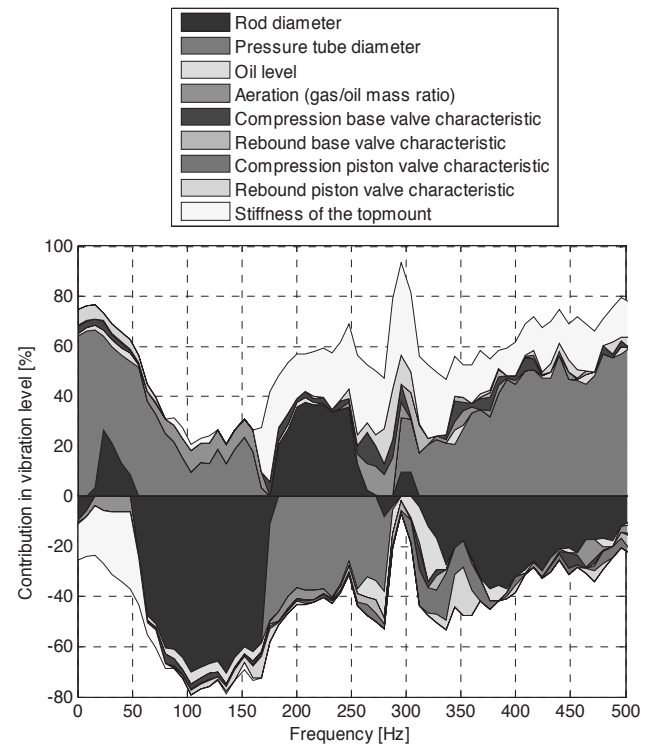


Fig. 5. Vibration contributors around the operating point

The high-range (30%) sensitivity analysis neglects the geometrical changes since they cannot be further considered independently (Fig. 6). Thus, the greatest influence has the topmount stiffness which influences the frequency 0-70Hz (decreasing) and 70-500Hz (increasing). Aeration effect and oil level mostly contribute in the frequency range 50-150Hz. Valve characteristics have moderate effect. The rebound and compression intake valve affect higher frequencies ($< +10\%$ & $> -10\%$). The piston compression valve has the greatest minimizing effect achieving up to -40% .

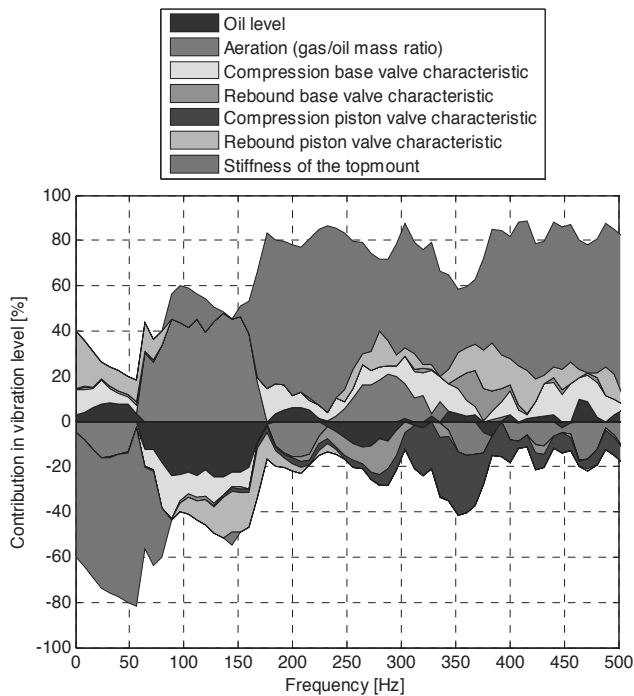


Fig. 6. Vibration contributors out of the operating point

5. Summary

The paper proposes and demonstrates a first-principle model-based approach towards minimizing vibrations of hydraulic dampers installed in passenger or commercial vehicles by means of sensitivity analysis. First-principle model offers physical insight and sufficient numerical performance to be applicable in understanding of vibration contributors (e.g. valve system, rod-bore combination, topmount stiffness).

The intended sensitivity analysis requires the accurate model capable to provide a response in a wide range of operating conditions which is well fitted to operational data. Adjusting a model to data is, in most cases, a non-convex optimization problem and the criterion function may have several local minima. It is therefore most natural to use physical insight to provide initial values to ensure robustness and fast convergence of the optimization process as well as to reduce the dimensionality of the parameters space by selecting only these parameters values of which are difficult to derive. Using physics-based initial conditions has significant advantage over blind (random) initialization of the optimization routine and furthermore, physical meaning of the parameters allows additional constraints to be set on the error function and/or model parameters narrowing the domain in which the optimum is being searched for. For example, the damping ratio in the model of the servo-valve system is limited in the range from zero to unity. Ranges of tunable model parameters constitute a hyper-cube in the so-called parameter space. The number of parameters defines dimensionality of such a space, for instance, if the model has two parameters, the

parameter space is two-dimensional and ranges of the parameters form a rectangle. Optimization problem is stated by giving the parameter space, a criterion function and a domain over which the function is defined. Solving an optimization problem means finding extrema of the criterion function that are located within the domain. Typically, it suffices to find a single extremum located within proximity of a given point in the domain, to which end an iterative optimization process can be used. Constructing the criterion function requires multiple observed data points to be available and, ideally, to be uniformly distributed covering the entire operating range. Validation of the model adjustment quality indicates a good correlation in the frequency domain between the simulations and measurements at a level of 0.8-0.9 by means of the Pearson correlation coefficient.

The sensitive analysis indicated the amplification and reduction vibration contributors by means of positive or negative changes in design and physical parameters. For example, the aeration effect is positively correlated with temperature of the hydraulic damper which is the consequence of its longer operation at higher strokes (heat energy dissipation). If aeration effect occurs, the acceleration of piston-rod assembly increases of 40% compare to no-aeration conditions. On the hand, if hydraulic stiffness of the compression piston valve characteristics is decreased (lower flow rate) than the piston-rod acceleration level is lowered by -40% at 350Hz.

6. Nomenclature

Latin characters

- $\equiv d/dt$ - the dot substitutes the time derivative
- A_{com} - the area of the piston section [m²]
- A_{reb} - the area of the rebound side of the piston
 $A_{reb} = A_{com} - A_{rod}$ [m²]
- A_{rod} - the area of the rod section [m²]
- c_{TM} - the top mount damping coefficient [N·s/m]
- F_d - the hydraulic damper force [N]
- F_{fric} - the dry friction force [N]
- $F_{fric\ max}$ - the maximal dry friction force [N]
- K - the bulk modulus of the oil [Pa]
- k_{TM} - the topmount stiffness [N/m]
- M - the molar mass of gas [kg/mol]
- m_{TM} - the moving mass of the piston-rod assembly of a hydraulic damper the topmount [kg]
- m_{com} - the mass of the oil-gas emulsion in the compression chamber [kg]
- m_{com_ini} - the initial mass of the oil-gas emulsion in the compression chamber [kg]
- m_{emu} - the mass of the oil-gas emulsion in whole double-tube damper
- m_{emu_res} - mass of the oil-gas emulsion in the reserve chamber [kg]
- m_{gas} - the mass of the gas (dissolved and non-dissolved in oil) [kg]
- m_{gas_res} - the mass of the free gas in the reserve chamber [kg]
- m_{oil} - the total mass of the oil inside the hydraulic damper [kg]
- m_{reb} - the mass of the oil-gas emulsion in the rebound chamber [kg]

m_{reb_ini}	- the initial mass of the oil-gas emulsion in the rebound chamber [kg]
m_{res}	- the mass of the oil-gas emulsion in the reserve chamber [kg]
p_0	- the atmospheric pressure $p_0=1e5$ [Pa]
p_{com}	- the pressure in the compression chamber [Pa]
p_{ini}	- the initial pressure in the hydraulic damper [Pa]
p_{reb}	- the pressure in the rebound chamber [Pa]
p_{res}	- the pressure in the reserve chamber [Pa]
$q_{piston,com}$	- the flow through the piston compression intake [m ³ /s]
$q_{cend,reb}$	- the flow through the base (cylinder-end) rebound intake [m ³ /s]
$q_{cend,com}$	- the flow through the base (cylinder-end) compression control valve [m ³ /s]
$q_{piston,reb}$	- the flow through the piston rebound control valve [m ³ /s]
q_{rg}	- the flow through rod-guide restriction [m ³ /s]
$\tanh(.)$	- the function of a hyperbolic tangent
V_{com}	- the volume of the compression chamber [m ³]
V_{com_ini}	- the initial volume of the compression chamber [m ³]
V_{emu_res}	- the volume of the oil-gas emulsion in the reserve chamber [kg/m ³]
V_{reb}	- the volume of the rebound chamber [m ³]
V_{reb_ini}	- the initial volume of the rebound chamber [m ³]
V_{res}	- the volume of the reserve chamber [m ³]
v_{ref}	- the reference velocity used in the dry friction model [m/s]
x_{rod}	- the displacement of the piston-rod assembly of the hydraulic damper [m]
x_{tube}	- the displacement of the tube of the hydraulic damper [m]
x_{TM}	- the displacement of the top mount [m]

Greek characters

$\Delta p_{com,reb}$	- the pressure drop between the compression and the rebound chamber [Pa]
$\Delta p_{com,res}$	- the pressure drop between the compression and the reserve chamber [Pa]
$\Delta p_{reb,com}$	- the pressure drop between the rebound and the compression chamber [Pa]
$\Delta p_{reb,res}$	- the pressure drop between the rebound and the reserve chamber [Pa]
$\Delta p_{res,com}$	- the pressure drop between the reserve and the compression chamber [Pa]
ρ_{com}	- the average density of the oil-gas emulsion in the compression chamber [kg/m ³]
ρ_{com,emu_res}	- density of the oil-gas emulsion that flows through rebound intake and compression control valve [kg/m ³]
ρ_{emu_res}	- the average density of the oil-gas emulsion in the reserve chamber [kg/m ³]
ρ_{gas_com}	- the density of the gas in the compression chamber [kg/m ³]
ρ_{gas_reb}	- the density of the gas in the rebound chamber [kg/m ³]
ρ_{gas_res}	- the density of the gas in the reserve chamber [kg/m ³]
ρ_{oil_com}	- the oil density in the compression chamber [kg/m ³]
ρ_{oil_reb}	- the oil density in the rebound chamber [kg/m ³]
ρ_{oil_res}	- the oil density in the reserve chamber [kg/m ³]
ρ_{reb}	- the average density of the oil-gas emulsion in the

rebound chamber [kg/m³]

$\rho_{com,reb}$ - density of the oil-gas emulsion that flows through compression intake and rebound control valve [kg/m³]

ρ_{res} - the average density of the oil-gas emulsion and free gas in the reserve chamber [kg/m³]

Acknowledgements

The authors gratefully acknowledge the financial support of the research project: N N502 087838 funded by the Polish Ministry of Science (MNI) and RGH-9/RMT0/2012 founded by Rector of Silesian Technical University.

References

- [1] M. Annarumma, A. Naddeo, M. Pappalardo, Software independence, impact on automotive product development process, Journal of Achievements in Materials and Manufacturing Engineering 31/2 (2008) 725-735.
- [2] K. Białas, Comparison of passive and active reduction of vibrations of mechanical systems, Journal of Achievements in Materials and Manufacturing Engineering 18 (2006) 455-458.
- [3] K. Białas, Synthesis of mechanical systems including passive or active elements reducing of vibrations, Journal of Achievements in Materials and Manufacturing Engineering 20 (2007) 323-326.
- [4] A. Buchacz, The synthesis of vibrating bar-systems represented by graph and structural numbers, Scientific Letters of Silesian University of Technology, Mechanics 104, Silesian University of Technology Press, 1991 (in Polish).
- [5] A. Buchacz, D. Gałęziowski, The Inverse task of discrete vibrating systems, Silesian University of Technology Press, 2012 (in Polish).
- [6] A. Buchacz, S. Żółkiewski, Dynamic analysis of the mechanical systems vibrating transversally in transportation, Journal of Achievements in Materials and Manufacturing Engineering 20 (2007) 331-334.
- [7] J. Świder, G. Wszolek, K. Foit, P. Michalski, S. Jendrysik, Example of the analysis of mechanical system vibrations in GRAFSIM and CATGEN software, Journal of Achievements in Materials and Manufacturing Engineering 20 (2007) 391-394.
- [8] P. Czop, D. Sławik, A high-frequency model of a shock absorber and servo-hydraulic tester, Mechanical Systems and Signal Processing 25/6 (2011) 1937-1955.
- [9] P. Czop, K. Kost, D. Sławik, G. Wszolek, Formulation and identification of first-principle data-driven models. Journal of Achievements in Materials and Manufacturing Engineering 44/2 (2011) 179-186.
- [10] P. Czop, D. Sławik, G. Wszolek, Demonstration of first-principle data-driven models using numerical case studies. Journal of Achievements in Materials and Manufacturing Engineering 45/2 (2011) 170-177.
- [11] L. Ljung, System identification - Theory for the user, Prentice-Hall, USA, 1999.
- [12] Matlab/Simulink package documentation, The Math Works Inc., Natick 1998.

- [13] J. Madar, J. Abonyi, F. Szeifert, Feedback linearizing control using hybrid neural networks identified by sensitivity approach, *Engineering Applications of Artificial Intelligence* 18/3 (2006) 343-351.
- [14] P. Czop, A. Skrobol, D. Sławik, G. Wszolek, A nonlinear, data-driven model applied in the design process of disc-spring valve systems used in hydraulic dampers, *SIMULATION Transactions of The Society for Modeling and Simulation International* 89/3 (2013) 419-431.
- [15] T. Dzitkowski, A. Dymarek, Design and examining sensitivity of machine driving systems with required frequency spectrum, *Journal of Achievements in Materials and Manufacturing Engineering* 26/1 (2008) 49-56.